

Wavy Ribbons of Carbon Nanotubes for Stretchable Conductors

Feng Xu, Xin Wang, Yuntian Zhu, and Yong Zhu*

Wavy ribbons of carbon nanotubes (CNTs) are embedded in elastomeric substrates to fabricate stretchable conductors that exhibit excellent performance in terms of high stretchability and small resistance change. A CNT ribbon with a thin layer of sputtered Au/Pd film is transferred onto a prestrained poly(dimethylsiloxane) (PDMS) substrate and buckled out-of-plane upon release of the prestrain. Embedded in PDMS, the wavy CNT ribbon is able to accommodate large stretching (up to the prestrain) with little change in resistance. For a prestrain of 100%, the resistance increases only about 4.1% when the wavy CNT ribbon is stretched to the prestrain. A simple stretchable circuit consisting of a light-emitting diode and two wavy ribbons is demonstrated and shows constant response on significant twisting, folding, or stretching. Fabricated with a simple buckling approach, the wavy CNT-ribbon-based stretchable conductors (e.g., interconnects and electrodes) could play an important role in stretchable electronics, sensors, photovoltaics, and energy storage.

1. Introduction

Materials that remain electrically conducting upon significant stretching, bending, twisting, and/or folding are critical for many new applications ranging from flexible displays^[1] and stretchable electronics^[2] to artificial muscles^[3] and comfortable skin sensors.^[4] Carbon nanotubes (CNTs) have high aspect ratios, excellent electric conductivity, high thermal stability, and mechanical robustness, which makes them promising materials for stretchable conductors.^[5] Several methods have been reported for the fabrication of CNT-based stretchable conductors. By mixing millimeter-long single-walled CNTs (SWNTs), an ionic liquid, and a fluorinated copolymer, rubber-like conductive composites were developed by Sekitani et al.^[6] that exhibited high conductivity and excellent stretchability. Other methods include depositing transparent SWNT films on polymer films,^[7] backfilling SWNT aerogels with polymers,^[8] infiltrating multiwalled CNT (MWNT) forests with polymer

binder,^[9] and dispersing MWNTs in polymers by ultrasonication or melt-shear mixing.^[10] Still, these materials/structures have several limitations, such as low conductivity,^[10] decreasing conductivity with applied strain,^[7,9,10] or complicated fabrication processes.^[6,8]

CNT ribbons drawn out from vertically grown CNT arrays have attracted much attention for a variety of applications due to their unique properties, such as being unidirectionally aligned, ultrathin, transparent, and conductive.^[11] Promising stretchable conductors have been fabricated by simply embedding single-layer^[12] or even-layer cross-stacked CNT ribbons^[13] in poly(dimethylsiloxane) (PDMS). However, these composite structures typically have moderate conductivity ($>200 \Omega \square^{-1}$ in sheet resistance), and their resistance increases substantially when stretched.

For the former structure, it was found that a series of several stretching/releasing cycles helped to stabilize the resistance under a certain strain range, although the operating principle remained elusive.^[12]

For stretchable conductors, another strategy is to fabricate wavy structures by releasing a prestrained elastomeric substrate with an upper layer of conductive materials.^[14] Following this strategy, both evaporation^[15] and solution processing^[16] have been utilized to fabricate wavy metal films as stretchable conductors. In addition, the buckling strategy has been employed to develop stretchable device components based on semiconductor nanoribbons,^[17] nanowires,^[18] and CNTs (randomly distributed and nontransparent).^[19] However, the buckling of CNT ribbons on elastomeric substrates has not been reported previously; it is unclear how the constituent CNTs would buckle (either collectively or individually). In addition, these CNT ribbons have relatively high sheet resistance;^[20] few studies have reported low enough resistance in the CNT ribbons such that they meet the requirements for practical device applications.^[21]

In this paper, we report the fabrication and performance of stretchable conductors based on buckled CNT ribbons. Reduced-resistance CNT ribbons were produced by sputtering a thin film of Au/Pd onto their surface. The metal-coated CNT ribbons were then transferred onto a prestrained PDMS substrate. Release of the prestrain led to periodic, out-of-plane buckling of the CNT ribbon. A stretchable conductor was constructed by coating the buckled CNT ribbon with a further thin layer of PDMS (the CNT ribbon was embedded in PDMS). The resistance of the

F. Xu, Prof. Y. Zhu
Department of Mechanical and Aerospace Engineering
North Carolina State University
Raleigh, NC 27695-7910, USA
E-mail: yong_zhu@ncsu.edu

X. Wang, Prof. Y. T. Zhu
Department of Materials Science and Engineering
North Carolina State University
Raleigh, NC 27695-7907, USA

DOI: 10.1002/adfm.201102032



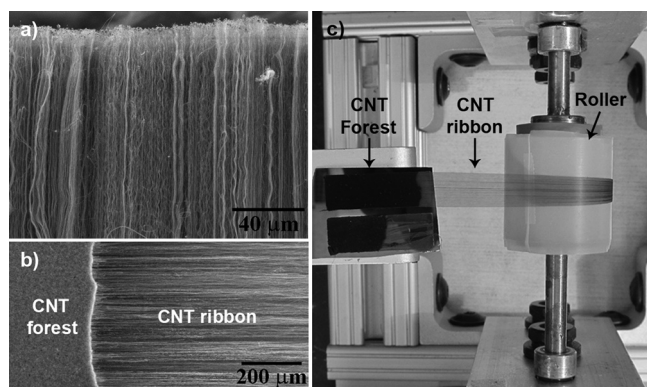


Figure 1. a) Side-view SEM image of the CNT forest. b) SEM image showing the ribbons directly drawn from the CNT forest. c) Photograph of the assembled apparatus used in our experiments to draw the CNT ribbons and attach them onto the teflon substrate.

conductor increased only about 4.1% when stretched to the pre-strain (100%). The buckled CNT ribbon exhibits markedly better performance (high stretchability and small resistance increase) than almost all stretchable conductors reported to date. Furthermore, a simple stretchable circuit composed of a light-emitting diode (LED) and two buckled CNT ribbons is demonstrated.

2. Results and Discussion

The CNT ribbons were drawn directly from spinnable vertically grown MWNT forests. **Figure 1a** shows a scanning electron microscopy (SEM) image of a CNT forest (side view), in which the CNTs are macroscopically straight and parallel. **Figure 1b** shows an SEM image (top view) of a ribbon being drawn from the CNT forest. It can be seen that the CNTs are uniformly aligned along the drawing direction. The diameters of the MWNTs in our study typically ranged from 30 to 50 nm. **Figure 1c** is an photograph showing the experimental setup used in the drawing process. With the assistance of a roller, the CNT ribbons were drawn and attached to a teflon substrate that was wrapped around the roller. High-purity alcohol was then dropped on the teflon substrate, which caused shrinkage of the film due to the surface tension effects from rapid evaporation.

Figure 2 shows schematically the fabrication process of buckled CNT ribbons. The conductivity of the CNT ribbon (sheet resistance of $211 \Omega \square^{-1}$) is mediocre for many applications such as liquid-crystal displays, so one step in our process is to coat the CNT/teflon substrate with a thin layer of Au/Pd alloy by magnetron sputtering (**Figure 2a**). After the coating step, the CNT/teflon substrate was brought into conformal contact with prestrained PDMS (**Figure 2b**). After brief contact (i.e., a few minutes), the teflon substrate was slowly peeled from the PDMS, and the CNT ribbon remained on the PDMS (**Figure 2c**). The successful transfer of the nanostructures from one substrate to another depends on the adhesion between the nanostructures and the substrates. Since PDMS has higher adhesion to CNTs than teflon, the CNT ribbon can be transferred from teflon to PDMS. Upon releasing the prestrained PDMS, the CNT ribbon buckled, as shown in **Figure 2d**.

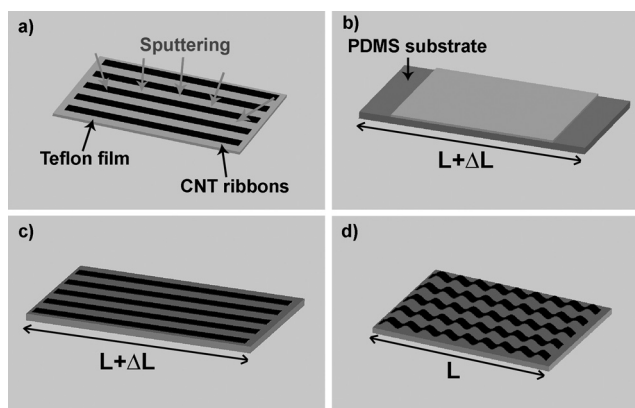


Figure 2. Schematic illustration of the process for fabricating the buckled CNT ribbons. a) Au/Pd alloy films were sputtered onto the CNT/teflon films. b) The teflon substrate sheet with CNT ribbons was brought into conformal contact with the prestrained PDMS. c) The CNT ribbons were left on the PDMS substrate after the teflon substrate was slowly peeled off the PDMS. d) The CNT ribbons buckled upon PDMS strain relaxation.

Table 1 lists the sheet resistance of CNT ribbons after being coated with Au/Pd films and transferred onto unstrained PDMS substrates. The sheet resistance decreased with as the thickness of the Au/Pd film increased. When the thickness of the metal coating reached 24 nm, the sheet resistance dropped to $72 \Omega \square^{-1}$. The coated metals were found to be distributed evenly on the CNTs, adding parallel conduction pathways around the outer surfaces of the nanotubes, and thus improving the conductivity of the ribbon.^[21] With further increase in the thickness of the metal film, the CNT ribbon was not completely transferred from the teflon substrate to the PDMS substrate, probably due to the enhanced bonding between the CNT ribbon and the teflon substrate. In fact, the CNT ribbons with 24 nm metal coating meet the requirements of conductivity for most real-world applications, such as touch screens ($500 \Omega \square^{-1}$) and liquid-crystal displays ($100 \Omega \square^{-1}$).^[21] Note that the transparency of the CNT ribbons was reduced by the metal coating because of the resulting increased CNT diameter. In our transfer process, the metal film coated on the teflon substrate (in the gaps between the CNTs) was not transferred. The transparency of the CNT ribbons could be improved either by adjusting the parameters of the CNT forests such as the height or diameters of the CNTs,^[20] or by trimming the as-drawn CNT ribbons by using oxygen plasma or laser trimming.^[21]

Table 1. Sheet resistance of the CNT ribbons on coating with an Au/Pd alloy layer. Typical errors are within 10% for the sheet resistance.

Sputtering time [s]	0	20	40	60	80
Coating thickness [nm]	0	8	16	24	32
Sheet resistance [$\Omega \square^{-1}$]	211	183	145	72	49 [failed to be transferred]

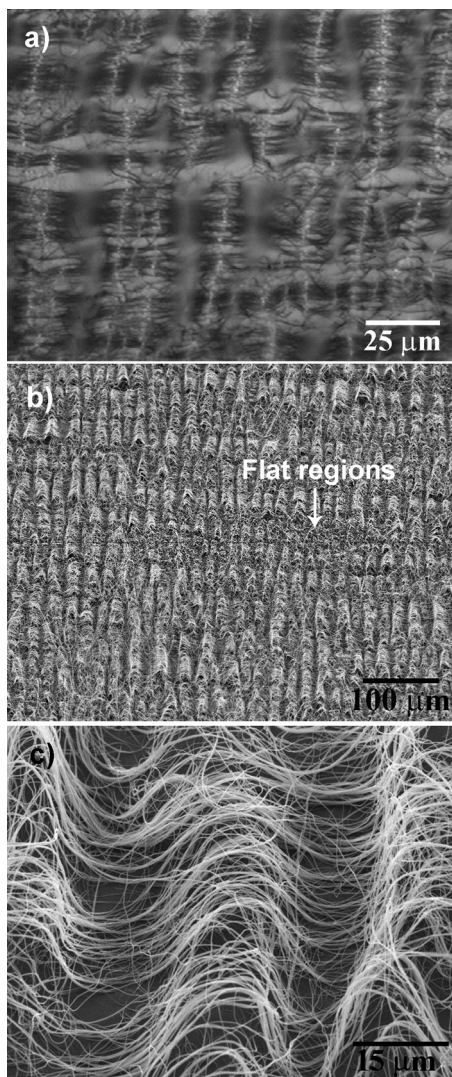


Figure 3. a) Top-view optical microscopy image of a CNT ribbon after releasing the strain of PDMS. b) Low- and c) high-magnification SEM images of the CNT ribbon after buckling. The images were taken by tilting the sample at an angle of 20°. Structural disorders other than a perfect, periodic, wavy structure (e.g., flat regions in contact with the substrate) can be seen.

Figure 3a shows the top-view optical microscopy image of a CNT ribbon after releasing the prestrained PDMS. Periodic dark areas distributed along the ribbon indicate the structural changes in the CNT ribbon. SEM images confirm that the ribbon buckled to form a periodic, wavy structure (Figures 3b,c). Interestingly, the CNT ribbon collectively shows an out-of-plane buckling that is different from the in-plane buckling of individual MWNTs on PDMS.^[22] The CNT ribbon also delaminated from the PDMS periodically. This is different from the buckling of randomly oriented CNT films,^[19] where wrinkling (no delamination) was observed because of the strong bonding between the CNTs and the PDMS (the bonding was intentionally enhanced by a post-purification process of the CNTs). But the post-purification process may potentially deteriorate the CNTs, thus influencing their conductivity. CNT ribbons represent a unique CNT

assembly in which individual millimeter-long CNTs are aligned and stacked along the length direction, forming a continuous film up to several meters long.^[12] The strong adhesion between the constituent CNTs within the ribbon makes the CNT ribbon behave like a thin solid film. The buckling mode of the CNT ribbons is determined by several factors, including the flexural rigidities of the ribbons and the PDMS, and adhesion between the ribbons and the PDMS. A similar buckling/delamination mode was observed for metal lines and lead zirconate titanate (PZT) ribbons on PDMS.^[23] A mechanics model was put forth to account for the competition between the buckle delamination mode and the wrinkling mode. In general, as the adhesion increases the wrinkling mode becomes favorable and vice versa. This model can be applied to the buckling of our CNT ribbons. Note that both the wavelength and amplitude of our buckled CNT ribbons were found to increase with the thickness of the metal coating, which is reasonable considering that the flexural rigidity of CNT ribbons increases with the thickness of the metal coating.

To fabricate a stretchable conductor, silver paste with a lead wire was used at each end of a buckled CNT ribbon (under a pre-strain of 100%) to serve as electrodes. Subsequently, a thin layer of uncured PDMS was cast on the top to enclose the device (as a result the CNT ribbon was embedded in PDMS). The top PDMS layer is useful for the stretchable conductor; it not only enhances the adhesion of the silver paste to the PDMS, but also protects the CNT ribbon from contamination. Finally, the whole device was baked in an oven at 65 °C for 12 h to cure the top PDMS. Figure 4a shows a fabricated stretchable conductor with a CNT ribbon embedded in PDMS (CNT/PDMS film). The conductor was placed on top of a piece of paper printed with “NCSU”, showing the transparency of the CNT ribbon. To test its performance as a stretchable conductor, the CNT/PDMS film was stretched by a tensile-testing stage (Ernest F. Fullam), while the electrical resistance was measured simultaneously. The increase in resistance of a representative CNT/PDMS film as a function of the applied strain is plotted in Figure 4b. The initial resistance of the CNT ribbon was 610 Ω. It can be seen that the resistance increased slowly with increasing tensile strain by only about 4.1% for up to 100% strain (the prestrain value). The buckled CNT ribbon exhibited far better performance (high stretchability and small resistance increase) than almost all stretchable conductors reported thus far.^[6–10,12,13] Upon release of the 100% strain, the resistance showed no obvious change and did not return to its initial state. The resistance variation was found to be within 1% in subsequent multiple stretching-and-releasing cycles with the maximum strain of 100%. However, when the strain exceeded the prestrain (100%), the resistance increased much more rapidly, showing a response similar to that of the unbuckled ribbons.^[12]

We have found previously that the resistance of buckled MWNTs remained nearly constant during a large range of tensile and compressive strains.^[22] The buckled CNT ribbon in this study is composed of a myriad of buckled MWNTs. When the ribbon is stretched, the dominant structural change is the straightening of the periodic, wavy structure (including individual CNTs and overlaps between them), which should cause no resistance change. In reality, slight disorders exist rather than a perfect, periodic, wavy structure (e.g., flat regions in contact with the substrate, as shown in Figures 3a and b). Similar flat regions were observed in the buckle-delaminated PZT ribbons on PDMS.^[23a] It is possible

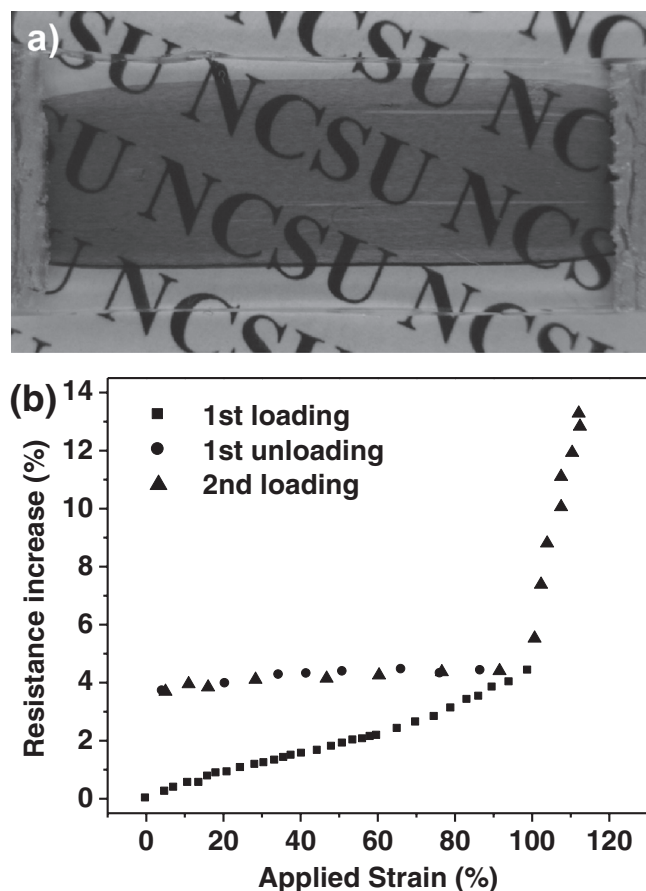


Figure 4. a) Photograph of the fabricated stretchable conductor with a buckled CNT ribbon embedded in PDMS. b) Resistance of a CNT/PDMS film as a function of tensile strains.

that CNT sliding happens in these regions during the stretching process, leading to the slightly increased resistance. Releasing the strain causes buckling of those CNTs; as a result, the resistance becomes nearly constant upon further stretching. When the applied strain exceeds the prestrain, the resistance increases rapidly due to sliding between all the straight CNTs.^[12]

To test the buckled CNT ribbons as stretchable conductors, we constructed a simple circuit consisting of an LED connected by two buckled CNT ribbons embedded in PDMS (with prestrain of 100%), as shown in **Figure 5**. The other ends of the ribbons were connected to a 3.6 V battery. **Figure 5a** shows a photograph of the device placed on top of a piece of paper with the LED turned on. The LED remained lit with the same illumination intensity while the CNT ribbon conductors were twisted by 360 degree (**Figure 5b**) or folded (**Figure 5c**). Even when the CNT ribbon conductors were stretched to a strain as large as 100%, the LED showed no noticeable change in illumination intensity (**Figure 5d** and **e**).

3. Conclusion

We have fabricated CNT-ribbon-based stretchable conductors following a simple buckling approach. The conductivity of the CNT ribbons was improved by sputtering Au/Pd films onto the surface

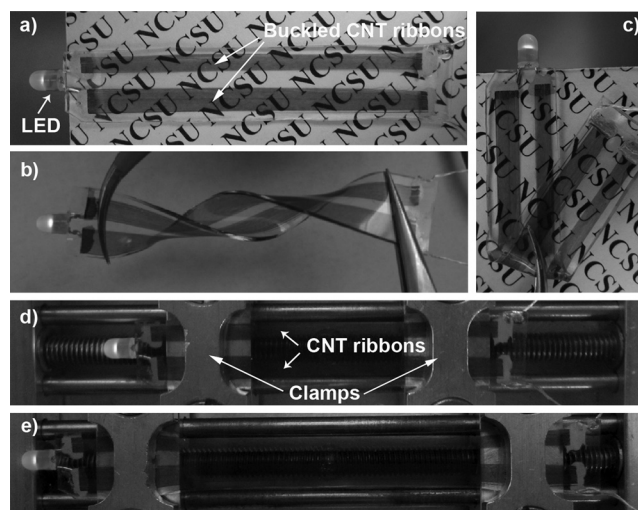


Figure 5. Performance of the LED integrated circuit as connected by two buckled-CNT-ribbon-based stretchable conductors. a) Photograph of the LED integrated circuit sitting on a piece of paper. b, c) Photograph of the LED integrated circuit under twisting and folding. d, e) Photograph of the LED integrated circuit under tensile strain of 0% and 100%. The two CNT ribbons are clamped on a mechanical testing stage.

of the CNT ribbons. The CNT ribbons were then transferred onto prestrained PDMS substrates. We found that CNT ribbons buckled out-of-plane upon release of the prestrain; the constituent CNTs buckled collectively. The resultant wavy ribbons (later embedded in PDMS) were able to accommodate large stretching (up to the prestrain, i.e., 100% in this study) and showed little increase in resistance. Further, a simple stretchable circuit consisting of an LED and two buckled ribbons was demonstrated. The LED did not show any observable change in illumination intensity when the CNT ribbons were stretched, folded, or twisted to a large extent. These buckled CNT ribbons exhibit far better performance (low resistance with metal coating, high stretchability, and small resistance increase) than almost all stretchable conductors reported to date. Together with an alternative manufacturing strategy we recently developed,^[22] the aligned CNT ribbons may find broad applications as stretchable interconnects and electrodes.

4. Experimental Section

MWNT Forests and PDMS Preparation: Vertically grown MWNT forests were synthesized by using a recently developed chloride-mediated chemical vapor deposition (CVD) method.^[24] PDMS substrates with thickness of 2 mm were prepared using Sylgard 184 (Dow Corning) by mixing the “base” and the “curing agent” at a ratio of 10:1. The mixture was first placed in a vacuum oven to remove air bubbles, and then thermally cured at 65 °C for 12 h. Rectangular slabs of suitable sizes were cut from the resultant cured piece.

Acknowledgements

This work was supported by the National Science Foundation under Award No. CMMI-1030637 (Clark Cooper, program director).

Received: August 26, 2011
Revised: November 26, 2011
Published online: January 19, 2012

- [1] G. H. Gelinck, H. E. A. Huitema, E. Van Veenendaal, E. Cantatore, L. Schrijnemakers, J. B. P. H. Van der Putten, T. C. T. Geuns, M. Beenhakkers, J. B. Giesbers, B. H. Huisman, E. J. Meijer, E. M. Benito, F. J. Touwslager, A. W. Marsman, B. J. E. Van Rens, D. M. De Leeuw, *Nat. Mater.* **2004**, *3*, 106.
- [2] a) J. A. Rogers, T. Someya, Y. G. Huang, *Science* **2010**, *327*, 1603; b) F. Xu, J. W. Durham, B. J. Wiley, Y. Zhu, *ACS Nano* **2011**, *5*, 1556.
- [3] A. E. Aliev, J. Y. Oh, M. E. Kozlov, A. A. Kuznetsov, S. L. Fang, A. F. Fonseca, R. Ovalle, M. D. Lima, M. H. Haque, Y. N. Gartstein, M. Zhang, A. A. Zakhidov, R. H. Baughman, *Science* **2009**, *323*, 1575.
- [4] V. Lumelsky, M. S. Shur, S. Wagner, *IEEE Sens. J.* **2001**, *1*, 41.
- [5] R. H. Baughman, A. A. Zakhidov, W. A. de Heer, *Science* **2002**, *297*, 787.
- [6] T. Sekitani, Y. Noguchi, K. Hata, T. Fukushima, T. Aida, T. Someya, *Science* **2008**, *321*, 1468.
- [7] L. B. Hu, W. Yuan, P. Brochu, G. Gruner, Q. B. Pei, *Appl. Phys. Lett.* **2009**, *94*, 161108.
- [8] K. H. Kim, M. Vural, M. F. Islam, *Adv. Mater.* **2011**, *23*, 2865.
- [9] M. K. Shin, J. Oh, M. Lima, M. E. Kozlov, S. J. Kim, R. H. Baughman, *Adv. Mater.* **2010**, *22*, 2663.
- [10] Y. Y. Huang, E. M. Terentjev, *Adv. Funct. Mater.* **2010**, *20*, 4062.
- [11] K. Jiang, J. Wang, Q. Li, L. Liu, C. Li, S. Fan, *Adv. Mater.* **2011**, *23*, 1154.
- [12] Y. Zhang, C. J. Sheehan, J. Zhai, G. Zou, H. Luo, J. Xiong, Y. T. Zhu, Q. X. Jia, *Adv. Mater.* **2010**, *22*, 3027.
- [13] K. Liu, Y. Sun, P. Liu, X. Lin, S. Fan, K. Jiang, *Adv. Funct. Mater.* **2011**, *21*, 2728.
- [14] N. Bowden, S. Brittain, A. G. Evans, J. W. Hutchinson, G. M. Whitesides, *Nature* **1998**, *393*, 146.
- [15] a) S. P. Lacour, J. Jones, S. Wagner, T. Li, Z. G. Suo, *Proc. IEEE* **2005**, *93*, 1459; b) S. P. Lacour, S. Wagner, Z. Y. Huang, Z. G. Suo, *Appl. Phys. Lett.* **2003**, *82*, 2404.
- [16] a) D. C. Hyun, M. Park, C. Park, B. Kim, Y. Xia, J. H. Hur, J. M. Kim, J. J. Park, U. Jeong, *Adv. Mater.* **2011**, *23*, 2946; b) X. Wang, H. Hu, Y. Shen, X. Zhou, Z. Zheng, *Adv. Mater.* **2011**, *23*, 3090.
- [17] a) D. Y. Khang, H. Q. Jiang, Y. Huang, J. A. Rogers, *Science* **2006**, *311*, 208; b) Y. G. Sun, W. M. Choi, H. Q. Jiang, Y. G. Y. Huang, J. A. Rogers, *Nat. Nanotechnol.* **2006**, *1*, 201.
- [18] a) F. Xu, W. Lu, Y. Zhu, *ACS Nano* **2011**, *5*, 672; b) S. Y. Ryu, J. L. Xiao, W. Il Park, K. S. Son, Y. Y. Huang, U. Paik, J. A. Rogers, *Nano Lett.* **2009**, *9*, 3214.
- [19] C. Yu, C. Masarapu, J. Rong, B. Wei, H. Jiang, *Adv. Mater.* **2009**, *21*, 4793.
- [20] K. L. Jiang, K. Liu, Y. H. Sun, L. Chen, C. Feng, X. F. Feng, Y. G. Zhao, S. S. Fan, *Nano Lett.* **2008**, *8*, 700.
- [21] C. Feng, K. Liu, J. S. Wu, L. Liu, J. S. Cheng, Y. Y. Zhang, Y. H. Sun, Q. Q. Li, S. S. Fan, K. L. Jiang, *Adv. Funct. Mater.* **2010**, *20*, 885.
- [22] Y. Zhu, F. Xu, *Adv. Mater.* DOI: 10.1002/adma.201103382.
- [23] a) Y. Qi, J. Kim, T. D. Nguyen, B. Lisko, P. K. Purohit, M. C. McAlpine, *Nano Lett.* **2011**, *11*, 1331; b) J. Song, Y. Huang, J. Xiao, S. Wang, K. C. Hwang, H. C. Ko, D.-H. Kim, M. P. Stoykovich, J. A. Rogers, *J. Appl. Phys.* **2009**, *105*, 123516.
- [24] a) Y. Inoue, K. Kakihata, Y. Hirono, T. Horie, A. Ishida, H. Mimura, *Appl. Phys. Lett.* **2008**, *92*, 2937082; b) Q. W. Li, X. F. Zhang, R. F. DePaula, L. X. Zheng, Y. H. Zhao, L. Stan, T. G. Holesinger, P. N. Arendt, D. E. Peterson, Y. T. Zhu, *Adv. Mater.* **2006**, *18*, 3160.